Landslide Detection with Ensemble-of-Deep Learning Classifiers Trained with Optimal Features

Abhijit Kumar, Rajiv Misra, T. N. Singh, and Vinay Singh

1 Introduction

Due to the force of gravity [1–4], soil, debris, and rocks slide down a slope, causing landslides. Multiple fatalities and large monetary losses are very common in the highlands and hills. There are also long-term consequences to its secondary risks. Landslide formation is influenced by a variety of environmental factors, including topography, lithology, land cover, and hydrology, according to some studies [5–8]. In addition to gravity, landslides may be triggered by rain, earthquakes, and human activity. With that being the case, it's vital to detect and anticipate landfalls' locations in order to avoid or minimize potential losses [9–12].

Quantitative predictive techniques for regional landslide spatial prediction have recently been published. Detailed geological field surveys may offer very accurate results when employing slope stability and landslide models. The issue is that effective physical modelling requires a wide variety of components, which is

A. Kumar (✉)
Department of Computer Science and Engineering, Indian Institute of Technology Patna,
School of Computer Science, University of Petroleum and Energy Studies Dehradun, Dehradun, IndiaPatna, India

R. Misra
Department of Computer Science and Engineering, Indian Institute of Technology Patna, Patna, India

T. N. Singh
Department of Computer Science and Engineering, Indian Institute of Technology Patna, Patna, India
Department of Earth Science, Indian Institute of Technology Bombay, Bombay, India

V. Singh
Department of Earth Science, Indian Institute of Technology Bombay, Bombay, India

R. Misra et al. (eds.), *Advances in Data Science and Artificial Intelligence*,
Springer Proceedings in Mathematics & Statistics 403,
https://doi.org/10.1007/978-3-031-16178-0_21

difficult to accomplish. This series has [13–16]. A new study has employed landslide susceptibility mapping (LSM), GIS, and remote sensing (RS) to evaluate the possible links between landslide conditions and the likelihood of occurrence. LSM can identify landslide-prone areas and build disaster mitigation and prevention strategies [17–19].

To assist LSM, many quantitative methods have been developed. Machine learning (ML) is increasingly being used in LSM because of its capacity to efficiently capture the correlations between landslides and environmental factors, such as logistic regression (LGR), support vector machines (SVMs), and decision trees (DTs), and random forests (RFs). However, classification by most methodologies does not reveal many characteristics of the causes of landslides. Deep learning methods such as DBN, RNN, and CNN, as well as convolutional neural networks, have become increasingly popular because of their ability to extract features (CNNs). In LSM's research, CNNs performed better in extracting spatial features than the others [24]. Twenty-five and a half. Landslide sampling, on the other hand, restricts the use of certain designs for feature extraction because of its data expression. There has been a lot of interest in deep learning approaches, which are capable of extracting features and capturing deep representations from large datasets. But, only a few hybrid models were used for the thorough usage of characteristics [26–29]. However, since most techniques only consider one feature dimension, they have poor generalizability in more complex situations. Hybrid methods are now in use that makes use of each approach's advantages for optimal feature utilization because of the complex nonlinear relationship of components and over-fitting.

2 Literature Review

To quantify landslide risk in Zichang City, China, Chen et al. [1] developed the bivariate statistical kernel logistic regression models PLKLR, PUKLR, and RBFKLR in 2021. It is now possible to create landslide susceptibility maps by comparing three landslide susceptibility maps and examining geographical trends. To begin, a 263 site historical landslide inventory was established. 263 landslide sites were used to train and test model assumptions and hypotheses. Second, 14 landslide conditioning variables were derived from the geographic data. Then, using frequency ratios, we investigated the relationship between the conditioning elements and landslide incidence. Then maps of landslide susceptibility were created using the normalized frequency ratios of the three models. Using correlation statistics, we looked at multi-collinearity. Researchers employed AUC comparison and validation to assess a model's predictive ability. As a result, quantitative comparisons of susceptibility maps are required to prevent over or underestimating factors (distance to the river and slope). The PUKLR model has AUC values of 0.884 and 0.766 for the training and validation datasets, respectively. The datasets were trained using RBFKLR and PLKLR models with AUCs of 0.879 and 0.797. These models were

used to verify and train datasets (AUC values of 0.758 and 0.752, respectively). The landslide susceptibility map may assist Zichang's decision-makers avoid future natural disasters.

In 2021, Zhang et al. [2] developed a deep learning system using spatial response characteristics and machine learning classifiers (SR-ML). There are three stages to the process. DSC collects geographical features to avoid confusing multi-factor data. Second, spatial pyramid pooling is used to obtain response characteristics of varied sizes (SPP). 3. High-level features are integrated with ML classifiers to enhance feature categorization. Examples of meaningful feature categorization using machine learning classifiers are provided in this framework. The Yarlung Zangbo Grand Canyon area gathered data on 203 landslides and 11 conditioning variables. The AUC for the suggested SR and SR-ML was 0.920 and 0.910, greater than the random forest (RF, with the largest AUC in ML group). Bigger landslide samples exhibited the lowest mean error (0.01), suggesting that LSM might benefit from utilizing larger landslide samples.

There will be an increased danger of earthquakes in the Zagros Mountains in Iran by 2021, according to Paryani et al. [3]. They used a combination of machine learning and metaheuristic algorithms, including the adaptive neuro-fuzzy inference system and the Harris hawks optimization (BA). Landslide data was divided in half using a 70/30 ratio for training and testing purposes. There were 14 landslide-related variables examined, and the stepwise weight assessment ratio (SWARA) was used to find the relationship between landslides and components. It was then used to create landslide susceptibility maps (LSMs) based on the hybrid models of ANFIS, HHO, SVR, SVR-HHO, and SVR-BA (LSMs). Lastly, two indices, namely MSE and AUROC, were utilized to compare and validate the models employed in the study. The AUROC values for the ANFIS-HHO, ANFIS-BA, SVR-HHO, and SVR-BA were 0.849, 0.82, 0.895, and 0.865, respectively, according to the validation results. With an AUROC of 0.895 and an MSE of 0.147, SVR-HHO was the most accurate while ANFIS-BA was the least accurate, both based on an AUROC value of 0.82. Based on the data, the SVR model is superior than the ANFIS model, and the HHO algorithm has beaten the bat approach in terms of performance. Property use planners may utilize the map created in this study to better manage their land.

Using computer-based sophisticated machine learning methodologies in the year 2021, Mandal et al. [4] built LSMs and compared the models' performance. A total of twenty factors, including both starting and contributing components, were examined in order to properly appreciate the landslide's spatial connection. One of the most popular machine learning techniques, convolutional neural network (CNN), was utilized to develop LSMs. Random forest (RF), artificial neural network model (ANN), and the bagging model were all used in conjunction with it. Landslide and non-landslide locations were randomly selected for training and validation datasets. The training and validation locations were selected in a ratio of 70:30. Multi-collinearity was assessed using the tolerance and variance inflation factor, while the information gain ratio was utilized to assess the significance of certain conditioning factors. Studies have shown a low degree of multi-collinearity when it comes to landslide conditioning factors, with rainfall being the most significant

contributor. Using each model's final prediction results, LSM was then split into five distinct categories, such as "very low," low, medium, high, and very high susceptibility. Based on the landslide susceptibility class distribution, more than 90% of the landslide area is vulnerable to landslides. According to the area under the receiver operating characteristics curve (ROC) curve and statistical methodologies such as RMSE and MAE were used to evaluate the models' accuracy (MAE). The CNN model achieved the highest AUC values in both datasets (training and validation): 0.903 and 0.939, respectively. As can be seen by the lower RMSE and MAE values, the CNN model performs better than other models. As a result, all models have performed well, but the CNN model has outperformed the other models in terms of accuracy.

With the use of sentinel-1D InSAR and MODIS data, Al-Najjar [5] hopes to demonstrate a method for predicting and mapping long-term and seasonal land surface deformation (subsidence/uplifting) and permafrost active layer thickness in Alaska's Donnelly Training Area (DTA) by the year 2020 (ALT). SAR images were compared for coherence (or resemblance) to see whether they could be used together. They were tested for their overall quality by conducting sensitivity analyses and an accuracy review. Seasonal subsidence in June and July was forecast to be in the range of 0–0.43%, whereas the predicted uplifting from September to May of the next year was predicted to be in the range of 0.34 m. DTA's southern and northern areas were expected to experience the majority of the long-term subsidence and rising (from 2015 to 2018). In the east river, west, and south, ALT estimates were greater, while those in the north were lower as a result of spatially variable time delays. For example, coherence estimates were considerably different from zero, and the average residual from ALT estimations was statistically indistinguishable from zero when compared to the referenced forecasts from a commonly used yearly prediction model. For seasonal surface deformation estimates, regional distributions of the uncertainties in model coefficient estimates, phase change estimates, modeling error estimates, and image pairs were similar. With the use of the InSAR pictures and MODIS data, this approach has been able to map and monitor permafrost changes in regions like DTA, where collecting field observations is difficult and costly. We also discovered that the DTA's permafrost deformation is very variable in terms of location and time, which enabled us to develop a near-real-time monitoring system for the permafrost environment.

3 Problem Statement

LSM depends on aerial picture interpretation and field verification, but gathering aerial photos is difficult [7, 8]. Researchers have gradually applied LDM to environmental monitoring using remote sensing (RS) [9–13]. Initially, high-resolution laser images were used to locate large-scale landslides [14, 15]. In modest shallow landslides, laser scans cannot detect A landslide's texture, color, and other features were compared to the surrounding ground objects in optical photographs.

WorldView [17], QuickBird [18], GaoFen-2 [19], IKONOS [20], and InSAR technologies are increasingly employed to LDM [21]. Both pixel-based and object-oriented techniques are used [22]. In this method, high-resolution photographs are used to identify landslides. These and other stages of landslide detection generate error accumulation and fluctuation in accuracy (ACC) [5, 23]. However, pixel-based LDM may solve these difficulties by simply identifying single-pixel [24, 25]. In addition, support vector machines (SVM), random forests (RF), decision trees (DT), and artificial neural networks (ANN) are used (ANN). Landslides may also be retrieved from optical images [30]. Others exploited the study area's attributes for LDM such as hydrology or evening light. However, most of the literature using RS images for LDM disregards landslide debris' morphological, geological, and other features. So we are worried about landslides. Convolutional neural networks (CNNs) can train a large number of parameters efficiently by utilizing weight sharing and other qualities. LeNet, AlexNet, GoogleNet, VGGNet, ResNet, and DenseNet are all deep neural network models based on the basic CNN model. Ces models excel in image classification. The CNN model is often utilized in landslide research. In landslide detection, its upgraded approach residual neural networks (ResNets) has demonstrated promising results. Due to the large amount of RS data employed, the preceding strategies need long model training durations and a large number of training parameters. DenseNets are narrow networks with few parameters, reducing model training time. DenseNet excels in medical image segmentation [16]. In landslide detection, DenseNet has limited applicability. An ensemble of deep learning classifiers is proposed.

4 Methodology

In this research work, a novel landslide detection model for GIS images will be introduced by following their major phases: (i) pre-processing, (ii) feature extraction (iii) feature selection, and (iv) classification. The captured images will be pre-processed via Gabor filtering. Subsequently, the features like GLCM based texture features, temperature-vegetative index-based characteristics, Brightness Index (BR), Normalized Difference Vegetation Index (NDVI) and Green Normalized Difference Vegetation Index (GNDVI), Red-over-Green difference (RGD),Vegetation index difference (VID), Brightness difference (BRD), NDI based features and coloration index features are extracted from the pre-processed data. The extracted features will be fused together, and among those features, the optimal ones will be selected via a new hybrid optimization model. The new hybrid optimization model will be the conceptual blend of the standard Teamwork Optimization Algorithm (TOA) [31] and Poor and rich optimization algorithm (PRO) [32]. Finally, the selected optimal features are subjected to the newly constructed ensemble-of-classifiers model. The ensemble-of-classifiers model is constructed with Recurrent Neural Network (RNN), Bi-LSTM, and Bi-GRU. All these classifiers are trained with the selected optimal features acquired with the new hybrid optimization model. The

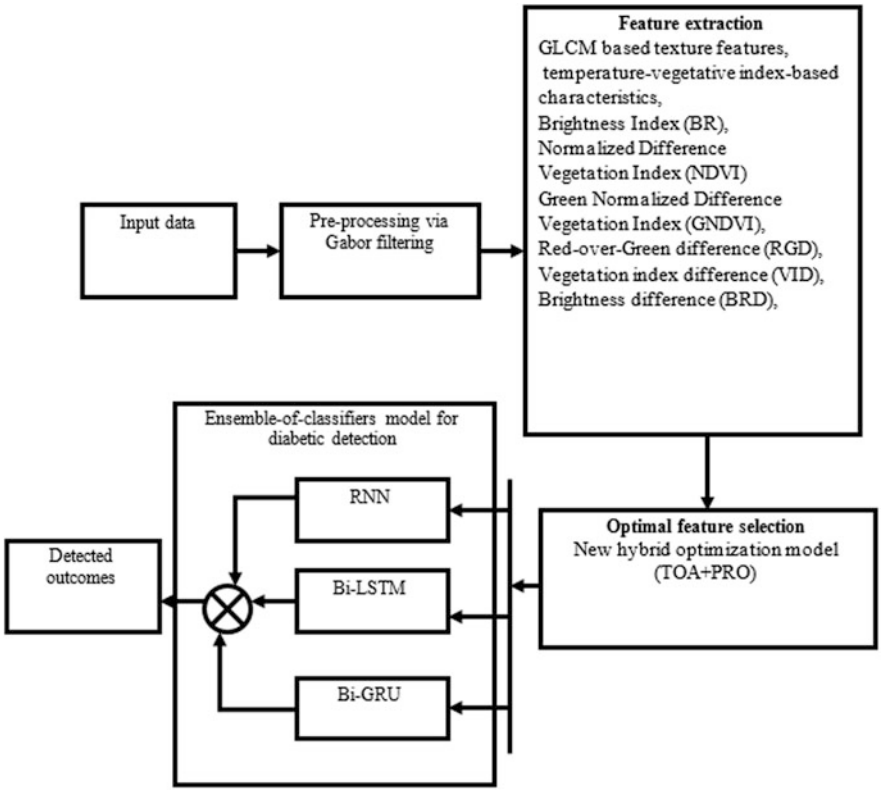

Fig. 1 The architecture of the projected model

ultimate outcome regarding the landslide forecasting will be acquired by fusing the outcomes acquired from RNN, Bi-LSTM and Bi-GRU as depicted in Fig. 1.

4.1 RNN

RNN is a type of neural network that has cyclic connections between its own nodes and is designed to mimic problems that a fully connected network cannot. Most neural networks, such as ANN and CNN, only build weight connections between layers; nodes between layers are disconnected, and nodes must be self-contained. In real life, however, many data are related to one another, necessitating a network model that can incorporate both prior and subsequent information, as well as handle data of any length at the same time. RNN was created to solve difficulties like these.

4.2 Bi-LSTM

The Bi-LSTM architecture consists of a forward LSTM and a reverse LSTM. The forward and backward layers both perform the usual LSTM function. The forward layer will compute a positive input sequence, whereas the backward layer will compute a reverse time sequence. The output of Bi-LSTMs can be described as a summation function of two hidden layer function outputs.

4.3 Bi-GRU

LSTM is proposed to tackle the "long dependencies" difficulties of regular RNNs, but it also fails to deal with very long-term and many dependencies. As a result, Bi-GRU is better suited to processing very lengthy dependencies since it may use both prior and subsequent data.

5 Results & Discussion

The proposed model has been tested in Python. The proposed model's performance has been compared to other existing models using Type I and Type II metrics. Negative predictive value (NPV), F1-Score, and Mathews correlation coefficient (MCC) are positive measurements whereas false-positive rate (FPR), false-negative rate (FNR), and false discovery rate (FDR) are negative measures.

The ultimate outcome regarding the landslide forecasting will be acquired by fusing the outcomes acquired from RNN, Bi-LSTM and Bi-GRU. The outcome acquired from RNN is out^{RNN} . The outcome acquired from Bi-LSTM is $\text{out}^{\text{Bi}-\text{LSTM}}$. The outcome acquired from Bi-GRU is $\text{out}^{\text{Bi}-\text{GRU}}$ the final outcome is

$$\text{out} = \frac{\text{out}^{\text{RNN}} + \text{out}^{\text{Bi-LSTM}} + \text{out}^{\text{Bi-GRU}}}{3}.$$

This outcome tells about the presence/absence of landslide in input GIS images.

An indication for evaluating the proposed prediction model's performance is introduced to compare the the mean square error (MSE), root mean square error (RMSE), standard deviation (SD) and mean error (ME) of the simulation results. Equations (1)–(4) illustrate RMSE, MSE, SD, and ME:

$$RMSE = \sqrt{\frac{\sum_{k=1}^{n} \left(y_k - \hat{y_k}\right)^2}{N}} \tag{1}$$

$$MSE = \frac{\sum_{k=1}^{n} \left(y_k - \hat{y_k}\right)^2}{N} \tag{2}$$

$$SD = \sqrt{\frac{1}{N}\sum_{k=1}^{n} (y_k - \mu)^2} \tag{3}$$

$$ME = \frac{1}{N}\sum_{k=1}^{n} \left(y_k - \hat{y_k}\right)^2 \tag{4}$$

Where n implies a number of sample data, μ implies the observed data's arithmetic mean, y_k represents $\hat{y_k}$ denotes the observation and prediction values.

6 Conclusion

We compared the ensemble-of-classifiers model to existing landslide detection methods using the same training and simulation parameters. The effectiveness of the ensemble of classifiers (RNN + Bi-LSTM + Bi-GRU) landslide detection system is compared with vanilla RNN + Bi-LSTM and RNN + Bi-GRU. The experiments proved that the proposed method has outperformed the RNN + Bi-LSTM and RNN + Bi-GRU both in terms of performance measures and robustness. With the hybrid optimization model, our network performs better, which achieves 87% Training Accuracy. The main problem that we faced is training images, which is a very time-consuming task. Our future work will focus on reducing the computational complexities of this landslide detection system.

References

1. Xi Chen, Wei Chena, "GIS-based landslide susceptibility assessment using optimized hybrid machine learning methods", CATENA, 2021
2. HuijuanZhang, YingxuSong, YueWang, "Combining a class-weighted algorithm and machine learning models in landslide susceptibility mapping: A case study of Wanzhou section of the Three Gorges Reservoir, China", Computers & Geosciences, 2021

3. Sina Paryani, Aminreza Neshat, Biswajeet Pradhan, "Improvement of landslide spatial modeling using machine learning methods and two Harris hawks and bat algorithms", The Egyptian Journal of Remote Sensing and Space Science, 2021
4. Kanu Mandal, Sunil Saha, Sujit Mandal, "Applying deep learning and benchmark machine learning algorithms for landslide susceptibility modelling in Rorachu river basin of Sikkim Himalaya, India" Geoscience Frontiers, 2021
5. Husam A. H, Al-Najjar, Biswajeet Pradhan, "Spatial landslide susceptibility assessment using machine learning techniques assisted by additional data created with generative adversarial networks", Geoscience Frontiers, 2020.
6. S. Chen, Z. Miao, L. Wu and Y. He, "Application of an Incomplete Landslide Inventory and One Class Classifier to Earthquake-Induced Landslide Susceptibility Mapping," in *IEEE Journal of Selected Topics in Applied Earth Observations and Remote Sensing*, vol. 13, pp. 1649–1660, 2020. https://doi.org/10.1109/JSTARS.2020.2985088.
7. H. Cai, T. Chen, R. Niu and A. Plaza, "Landslide Detection Using Densely Connected Convolutional Networks and Environmental Conditions," in *IEEE Journal of Selected Topics in Applied Earth Observations and Remote Sensing*, vol.14, pp. 5235–5247, 2021. https://doi.org/10.1109/JSTARS.2021.3079196.
8. N. Shen *et al*., "Short-Term Landslide Displacement Detection Based on GNSS Real-Time Kinematic Positioning," in *IEEE Transactions on Instrumentation and Measurement*, vol. 70, pp. 1–14, 2021, Art no. 1004714. https://doi.org/10.1109/TIM.2021.3055278
9. B. Pradhan, H. A. H. Al-Najjar, M. I. Sameen, M. R. Mezaal and A. M. Alamri, "Landslide Detection Using a Saliency Feature Enhancement Technique From LiDAR-Derived DEM and Orthophotos," in *IEEE Access*, vol. 8, pp. 121942–121954,2020. https://doi.org/10.1109/ACCESS.2020.3006914
10. T. Liu, T. Chen, R. Niu and A. Plaza, "Landslide Detection Mapping Employing CNN, ResNet, and DenseNet in the Three Gorges Reservoir, China," in *IEEE Journal of Selected Topics in Applied Earth Observations and Remote Sensing*, vol.14, pp.11417–11428, 2021. https://doi.org/10.1109/JSTARS.2021.3117975
11. Z. Y. Lv, W. Shi, X. Zhang and J. A. Benediktsson, "Landslide Inventory Mapping From Bitemporal High-Resolution Remote Sensing Images Using Change Detection and Multiscale Segmentation," in *IEEE Journal of Selected Topics in Applied Earth Observations and Remote Sensing*, vol. 11, no. 5, pp. 1520–1532, May 2018. https://doi.org/10.1109/JSTARS.2018.2803784
12. Y. Yi and W. Zhang, "A New Deep-Learning-Based Approach for Earthquake-Triggered Landslide Detection From Single-Temporal RapidEye Satellite Imagery," in *IEEE Journal of Selected Topics in Applied Earth Observations and Remote Sensing*, vol. 13, pp. 6166–6176, 2020. https://doi.org/10.1109/JSTARS.2020.3028855
13. W. Shi and P. Lu, "Intelligent Perception of Coseismic Landslide Migration Areas Along Sichuan–Tibet Railway," in *IEEE Journal of Selected Topics in Applied Earth Observations and Remote Sensing*, vol. 14, pp. 8876–8883, 2021. https://doi.org/10.1109/JSTARS.2021.3105671
14. W. Shi, M. Zhang, H. Ke, X. Fang, Z. Zhan and S. Chen, "Landslide Recognition by Deep Convolutional Neural Network and Change Detection," in *IEEE Transactions on Geoscience and Remote Sensing*, vol. 59, no. 6, pp. 4654–4672, June 2021. https://doi.org/10.1109/TGRS.2020.3015826
15. B. Fang, G. Chen, L. Pan, R. Kou and L. Wang, "GAN-Based Siamese Framework for Landslide Inventory Mapping Using Bi-Temporal Optical Remote Sensing Images," in *IEEE Geoscience and Remote Sensing Letters*, vol. 18, no. 3, pp. 391–395, March 2021. https://doi.org/10.1109/LGRS.2020.2979693
16. M. I. Sameen and B. Pradhan, "Landslide Detection Using Residual Networks and the Fusion of Spectral and Topographic Information," in *IEEE Access*, vol. 7, pp. 114363–114373, 2019. https://doi.org/10.1109/ACCESS.2019.2935761

17. S. L. Ullo *et al*., "A New Mask R-CNN-Based Method for Improved Landslide Detection," in *IEEE Journal of Selected Topics in Applied Earth Observations and Remote Sensing*, vol. 14, pp. 3799–3810, 2021. https://doi.org/10.1109/JSTARS.2021.3064981
18. M. Zhang, W. Shi, S. Chen, Z. Zhan and Z. Shi, "Deep Multiple Instance Learning for Landslide Mapping," in *IEEE Geoscience and Remote Sensing Letters*, vol. 18, no. 10, pp. 1711–1715, Oct. 2021. https://doi.org/10.1109/LGRS.2020.3007183
19. M. Q. Pham, P. Lacroix and M. P. Doin, "Sparsity Optimization Method for Slow-Moving Landslides Detection in Satellite Image Time-Series," in *IEEE Transactions on Geoscience and Remote Sensing*, vol. 57, no. 4, pp. 2133–2144, April 2019. https://doi.org/10.1109/TGRS.2018.2871550
20. Q. Huang, C. Wang, Y. Meng, J. Chen and A. Yue, "Landslide Monitoring Using Change Detection in Multitemporal Optical Imagery," in *IEEE Geoscience and Remote Sensing Letters*, vol. 17, no. 2, pp. 312–316, Feb. 2020. https://doi.org/10.1109/LGRS.2019.2918254
21. B. Zhang and Y. Wang, "An Improved Two-Step Multitemporal SAR Interferometry Method for Precursory Slope Deformation Detection Over Nanyu Landslide," in *IEEE Geoscience and Remote Sensing Letters*, vol. 18, no. 4, pp. 592–596, April 2021. https://doi.org/10.1109/LGRS.2020.2981146
22. G. Yao *et al*., "An Empirical Study of the Convolution Neural Networks Based Detection on Object With Ambiguous Boundary in Remote Sensing Imagery—A Case of Potential Loess Landslide," in *IEEE Journal of Selected Topics in Applied Earth Observations and Remote Sensing*, vol. 15, pp. 323–338, 2022 https://doi.org/10.1109/JSTARS.2021.3132416
23. L. Nava, O. Monserrat and F. Catani, "Improving Landslide Detection on SAR Data Through Deep Learning," in *IEEE Geoscience and Remote Sensing Letters*, vol. 19, pp. 1–5, 2022, Art no. 4020405. https://doi.org/10.1109/LGRS.2021.3127073
24. F. K. Sufi and M. Alsulami, "Knowledge Discovery of Global Landslides Using Automated Machine Learning Algorithms," in *IEEE Access*, vol. 9, pp. 131400–131419, 2021, https://doi.org/10.1109/ACCESS.2021.3115043
25. C. Ye *et al*., "Landslide Detection of Hyperspectral Remote Sensing Data Based on Deep Learning With Constrains," in *IEEE Journal of Selected Topics in Applied Earth Observations and Remote Sensing*, vol. 12, no. 12, pp. 5047–5060, Dec.2019. https://doi.org/10.1109/JSTARS.2019.2951725
26. Z. Lv, T. Liu, X. Kong, C. Shi and J. A. Benediktsson, "Landslide Inventory Mapping With Bitemporal Aerial Remote Sensing Images Based on the Dual-Path Fully Convolutional Network," in *IEEE Journal of Selected Topics in Applied Earth Observations and Remote Sensing*, vol. 13, pp. 4575–4584, 2020. https://doi.org/10.1109/JSTARS.2020.2980895
27. J. Liu, D. Chen, Y. Wu, R. Chen, P. Yang and H. Zhang, "Image Edge Recognition of Virtual Reality Scene Based on Multi-Operator Dynamic Weight Detection," in *IEEE Access*, vol. 8, pp. 111289–111302, 2020. https://doi.org/10.1109/ACCESS.2020.3001386
28. T. Lei, Y. Zhang, Z. Lv, S. Li, S. Liu and A. K. Nandi, "Landslide Inventory Mapping From Bitemporal Images Using Deep Convolutional Neural Networks," in *IEEE Geoscience and Remote Sensing Letters*, vol. 16, no. 6, pp. 982–986, June2019. https://doi.org/10.1109/LGRS.2018.2889307
29. L. Zhiyong, T. Liu, R. Y. Wang, J. A. Benediktsson and S. Saha, "Automatic Landslide Inventory Mapping Approach Based on Change Detection Technique With Very-High-Resolution Images," in *IEEE Geoscience and Remote Sensing Letters*, vol. 19, pp. 1–5, 2022, Art no. 6000805. https://doi.org/10.1109/LGRS.2020.3041409
30. C. Ren, H. Shang, Z. Zha, F. Zhang and Y. Pu, "Color Balance Method of Dense Point Cloud in Landslides Area Based on UAV Images," in *IEEE Sensors Journal*, vol. 22, no. 4, pp. 3516–3528, 15 Feb.15, 2022. https://doi.org/10.1109/JSEN.2022.3141936
31. Mohammad Dehghani and Pavel Trojovský,"Teamwork Optimization Algorithm: A New Optimization Approach for Function Minimization/Maximization", Sensors, 2021
32. Seyyed Hamid, SamarehMoosavi, VahidKhatibi, Bardsiri,"Poor and rich optimization algorithm: A new human-based and multi populations algorithm", Engineering Applications of Artificial Intelligence, Vol.86, PP.165–181, 2019.